Discrimination of Healthy and Neoplastic Human Colon Tissues by ex Vivo HR-MAS NMR Spectroscopy and Chemometric Analyses

ARTICLE *in* JOURNAL OF PROTEOME RESEARCH · MAY 2009

Impact Factor: 4.25 · DOI: 10.1021/pr801094b · Source: PubMed

10 AUTHORS, INCLUDING:

Valeria Righi
University of Bologna
37 PUBLICATIONS **370** CITATIONS
SEE PROFILE

Marina Cocchi
Università degli Studi di Modena e Reggio …
115 PUBLICATIONS **1,474** CITATIONS
SEE PROFILE

Adele Mucci
Università degli Studi di Modena e Reggio …
138 PUBLICATIONS **1,726** CITATIONS
SEE PROFILE

Luisa Schenetti
Università degli Studi di Modena e Reggio …
146 PUBLICATIONS **1,825** CITATIONS
SEE PROFILE

research articles Journal of proteome research

Discrimination of Healthy and Neoplastic Human Colon Tissues by *ex Vivo* HR-MAS NMR Spectroscopy and Chemometric Analyses

Valeria Righi,[†,‡] Caterina Durante,[‡] Marina Cocchi,[‡] Carlo Calabrese,[#] Giulio Di Febo,[#] Ferdinando Lecce,[||] Annamaria Pisi,[§] Vitaliano Tugnoli,[†] Adele Mucci,[‡] and Luisa Schenetti*[,‡]

Dipartimento di Biochimica "G. Moruzzi", Università di Bologna, Via Belmeloro 8/2, 40126 Bologna, Italy, Dipartimento di Chimica, Università di Modena e Reggio Emilia, Via G. Campi 183, 41100 Modena, Italy, Dipartimento di Medicina Interna e Gastroenterologia, Università di Bologna, Via G. Massarenti 9, 40138, Bologna, Italy, Dipartimento Emergenza/Urgenza, Chirurgia Generale e dei Trapianti, Università di Bologna, Via G. Massarenti 9, 40138 Bologna, Italy, and DiSTA, Università di Bologna, Viale Fanin 44, 40100 Bologna, Italy

Received September 23, 2008

The metabolic profile of human healthy and neoplastic colorectal tissues was obtained using *ex vivo* High-Resolution Magic Angle Spinning (HR-MAS) NMR spectroscopy. Principal Components Analysis (PCA) and Partial Least Squares Discriminant Analysis (PLS-DA) were applied to NMR data in order to highlight the biochemical differences between healthy and neoplastic colorectal tissues. The synergic combination of *ex vivo* HR-MAS NMR spectroscopy with Multivariate Data Analysis enables discrimination between healthy and tumoral colorectal tissues and identification of the increase of taurine, acetate, lactate, and lipids, and the decrease of polyols and sugars as tumoral characteristics. Moreover, it was found that macroscopically/histologically normal colorectal tissues, collected at least 15 cm from the adenocarcinoma, are characterized by a metabolic pattern quite similar to that typical of tumoral lesions. It was shown that *ex vivo* HR-MAS NMR spectroscopy, performed on intact specimens, may be of great potentiality in the clinical evaluation of human neoplastic colorectal tissues and that the biochemical data represent the molecular basis for an accurate and noninvasive clinical applications of *in vivo* NMR spectroscopy.

Keywords: healthy colorectal • cancer colorectal • *ex vivo* High-Resolution Magic-Angle Spinning NMR spectroscopy • biochemical markers • Principal Component Analysis • Partial Least Squares Discriminant Analysis

Introduction

Colorectal cancer (CRC) is a very common cancer with high morbidity and mortality. The majority of colorectal cancers develop from pre-existing polyps.[1] The so-called adenoma-carcinoma path is well-established and it is estimated that 5% of polyps become malignant over a period of 5−10 years. Currently, there are four tests for the early detection of CRC, including fecal occult blood testing (FOBT), sigmoidoscopy (SIG), colonoscopy (COL), and double contrast barium enema (DCBE).[2−4] Recently, it has been reported that Magnetic Resonance Colonography is a feasible and promising method for detecting, with high accuracy, colorectal polyps and adenocarcinomas.[5,6]

In vivo Nuclear Magnetic Resonance spectroscopy (*in vivo* NMR) has been widely applied in biomedical research, with particular attention to molecular evaluations regarding diagnosis, treatment, and prognosis of a wide variety of human neoplasms.[7−9] Dzik-Jurasz et al.[10] first demonstrated the feasibility of *in vivo* ^{1}H NMR in locally advanced human colorectal adenocarcinomas, overcoming complications arising from tissue/air interface, thin dimension of the colon, its convoluted shape, and peristalsis. The authors reported that the most commonly detected metabolites were choline and lipid. The clinical application of *in vivo* NMR requires the identification of the overall metabolic profiles of colorectal tissues. Nowadays, *ex vivo* High-Resolution Magic Angle Spinning (HR-MAS) ^{1}H NMR spectroscopy provides detailed metabolic maps of intact tissue samples. *Ex vivo* HR-MAS NMR spectroscopy has been applied to characterize different human intact tissues such as brain,[11−19] breast,[20−22] prostate,[23−25] kidney,[26−28] cervix,[29,30] heart,[31] and stomach.[32−34] To our knowledge, only three HR-MAS NMR studies have been reported, one on rectal cancer[35] and two on the variation of the metabolic profile in healthy human gastrointestinal tract (GIT).[36,37] Nicholson et al. have reported topographical variation in the metabolic profiles of the human GIT and they

* Corresponding author: Luisa Schenetti, Università di Modena e Reggio Emilia, Dipartimento di Chimica, Via G. Campi 183, 41100 Modena, Italy. E-mail, luisa.schenetti@unimore.it; phone, (+39)0592055076; fax, (+39)059373543.
† Dipartimento di Biochimica "G. Moruzzi", Università di Bologna.
‡ Dipartimento di Chimica, Università di Modena e Reggio Emilia.
# Dipartimento di Medicina Interna e Gastroenterologia, Università di Bologna.
|| Dipartimento Emergenza/Urgenza, Chirurgia Generale e dei Trapianti, Università di Bologna.
§ DiSTA, Università di Bologna.

10.1021/pr801094b CCC: $40.75

Published on Web 02/05/2009

Table 1. Demographic, Histological Data, and Sample Labels[a]

patients (*n*)	age	sex	type	histology
Control subjects (9)	60.9 ± 8.6	3 male	normal	normal
Adenocarcinomas (14)	63.3 ± 9.2	7 male	adenocarcinomas	2 D (c10t, c15t) 8 MD (c11t, c12t, c14t, c16t, c17t, c20t, c21t, plus a test sample) 4 PD (c13t, c18t, plus two test samples)
			macroscopically normal mucosa*	normal

[a] (*)Obtained at least 15 cm from the adenocarcinoma from the same patients; D, differentiated; MD, mild differentiated; PD, poorly differentiated.

attribute them to the functional variation of the different regions of the gut.[36,37] In particular, the colon was found to have high levels of acetate, glutamate, inositols, and lactate and low levels of creatine, glycerophosphorylcholine, and taurine.[36]

The abundance of chemical data usually encompassed in the HR-MAS NMR spectra of biological samples requires the use of pattern recognition methods, that is, multivariate statistical methods, to extract metabonomic information correctly.[38−40] In general, two main issues have been addressed: the choice of proper spectral data preprocessing[41,42] and the efficacy of the presentation of results from the point of view of spectroscopic interpretation.[39,43,44] As far as the data analysis protocol is concerned, it usually includes an explorative step (mainly by Principal Component Analysis, PCA) followed by a classification/discrimination step, the most used methods being Partial Least Squares-Discriminant Analysis (PLS-DA) and OPLS-DA.

Here, we report a study on *ex vivo* HR-MAS NMR of healthy and neoplastic colorectal tissues in combination with multivariate methods, PCA[45] and PLS-DA.[46] Monodimensional and bidimensional NMR experiments were used to obtain the metabolic profile and identify the metabolites characterizing the colorectal tissues. PCA was carried out as explorative analysis in order to obtain an overview on the whole data set without forcing any model, and to extract relevant information. PLS-DA was used to build a classification model able to separate the classes of healthy and neoplastic human colorectal tissues based on their *ex vivo* HR-MAS NMR spectra. The results show that the synergic combination of NMR spectroscopy with chemometric techniques offers a useful tool to understand better some molecular aspects of colon tumor, as well as identify tumoral markers. Noteworthy, we show that macroscopically/histologically normal colon tissues collected far from the adenocarcinomas are characterized by a metabolic pattern similar to that typical of the tumoral lesions.

Materials and Methods

Sample Collection and Histologic Evaluation. Samples of 23 subjects, 14 affected by colorectal cancer (7 men, range 52−78 years, and 7 women, range 48−90 years), and 9 healthy (3 men, range 46−64 years, and 6 women, range 61−75 years) were evaluated. Five biopsies, four for histologic evaluation and one for NMR analysis, were taken from each subject during endoscopy. The specimen (biopsies and surgical samples) in patients with colon cancer were obtained exclusively from the carcinoma site, assuring the absence of any contaminants. Moreover, macroscopically normal colon specimens, taken at least 15 cm from the adenocarcinomas, were also collected from all unhealthy patients, and classified as normal by histological analysis.

Four specimens from each of the 23 patients were routinely fixed with 10% buffered formalin and embedded in paraffin, and serial sections were cut 2 to 3 mm thick. Adenocarcinomas were classified as well-differentiated (D), mildly differentiated (MD), and poorly differentiated (PD). Demographic, histological data, and sample labels are reported in Table 1. The tissue samples for NMR analyses were immediately put in liquid nitrogen, after endoscopy or surgery, and stored at −80 °C.

The study was approved by the local ethics committee. All patients received detailed information regarding the procedure and written informed consent was obtained.

Nuclear Magnetic Resonance Spectroscopy. Each sample, before NMR examination, was flushed with deuterated water (D_2O) to remove the residual blood, improve the homogeneity, water suppression, and add deuterium as nucleus for the lock system. The samples, 15−25 mg, were placed into a MAS zirconia rotor (4 mm o.d.), adjusted to 50 μL using the proper insert and then transferred into the probe cooled to 4 °C. ^{1}H and ^{13}C HR-MAS NMR spectra were recorded with a Bruker Avance400 spectrometer operating at 400.13 and 100.61 MHz, respectively. The instrument was equipped with a ^{1}H,^{13}C HR-MAS probe whose temperature was controlled by a Bruker Cooling Unit, and all the experiments were performed at 4 °C, to prevent tissue degradation processes, which are more evident at room temperature.[47] It takes about 20 min to set up the samples and instrument. Samples were spun at 4000 Hz and three different types of monodimensional (1D) proton spectra were acquired by using (i) a composite pulse sequence (zgcppr)[48] with 1.5 s water-presaturation during relaxation delay, 8 kHz spectral width, 32k data points, 32−64 scans; (ii) a water-suppressed spin−echo Carr−Purcell−Meiboom−Gill sequence (CPMGpr)[49] with 1.5 s water presaturation during relaxation delay, 1 ms echo time (τ), and 360 ms total spin−spin relaxation delay ($2n\tau$), 8 kHz spectral width, 32k data points, 128 scans; and (iii) a sequence for diffusion measurements based on stimulated echo and bipolar-gradient pulses (ledbpgp2s1d)[50] with big delta 200 ms, eddy current delay T_e 5 ms, little delta 2*2 ms, sine-shaped gradient with 32 G/cm followed by a 200 μs delay for gradient recovery, 8 kHz spectral width, 8k data points, 256 scans. Two-dimensional (2D) ^{1}H,^{1}H-COrrelation SpectroscopY (COSY)[51,52] spectra were acquired using a standard pulse sequence (cosygpprqf) and 0.5 s water-presaturation during relaxation delay, 8 kHz spectral width, 4k data points, 32 scans per increment, 128 increments. Two-dimensional ^{1}H,^{1}H-TOtal Correlation SpectroscopY (TOCSY)[53,54] spectra were acquired using a standard pulse sequence (mlevphpr) and 0.5 s water-presaturation during relaxation delay, 100 ms mixing (spin-lock) time, 4 kHz spectral width, 4k data points, 32 scans per increment, 128 increments. Two-dimensional ^{1}H,^{13}C-Heteronuclear Single Quantum Coherence

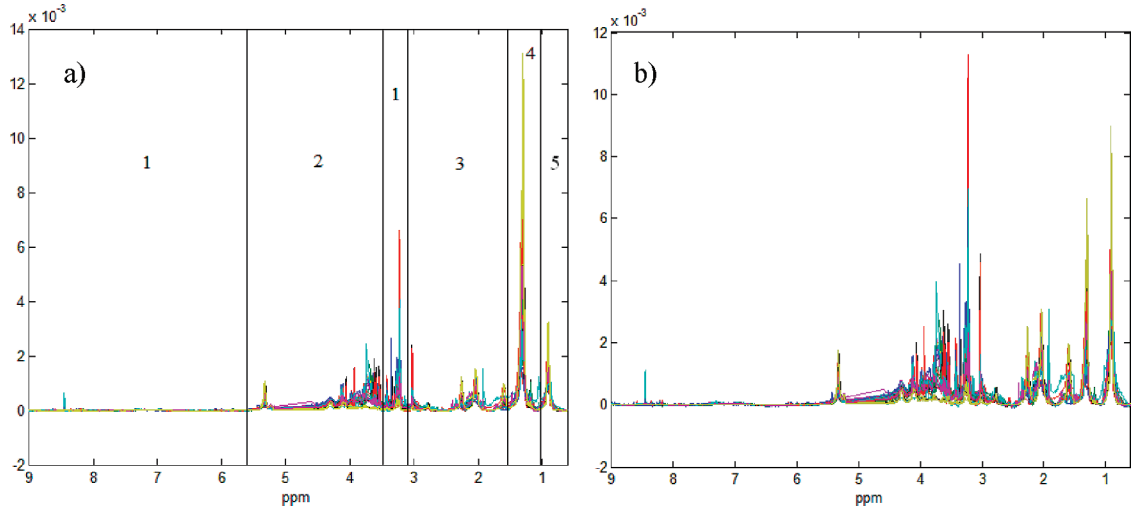

Figure 1. (a) Baseline-corrected and normalized NMR spectra. The vertical lines highlight the five regions selected for performing the block-scaling pretreatment; (b) the corresponding 'blockscaled' signals.

(HSQC)[55] spectra were acquired using a standard echo−antiecho pulse sequence (hsqcedetgp) and 0.5 s relaxation delay, 1.725 ms evolution time, 4 kHz spectral width in f_2, 4k data points, 128 scans per increment, 17 kHz spectral width in f_1, 256 increments.

Data Handling and Pretreatment. HR-MAS ^{1}H NMR data (standard ^{1}H sequence with water-presaturation) were processed by using the Bruker software, by applying 0.5 Hz line broadening prior to Fourier transformation, phased and baseline corrected (polynomial of order 6). The spectra acquired on human colon tissues are referenced to the chemical shift of the CH_3 peak of alanine at δ 1.48 ppm.

The NMR data points were reduced from 32k to 16k. The selected spectral width spans from δ 9.05 ppm to δ 0.05 ppm and the number of data points is 7500. The regions corresponding to water and polyethylene glycol (PEG) signals between δ 5.03−4.69 ppm and δ 3.75−3.68 ppm, respectively, were removed (6341 final data points), since these were regions of high variance, mainly due to sample acquisition/manipulation, not interesting from the point of view of healthy-neoplastic tissues discrimination.

Pretreatment of data is a critical and case-dependent issue in multivariate analyses, as far as NMR spectra are concerned. In this study, several preprocessings were tested and the best performance was obtained by normalizing each spectrum to the sum of the intensity data.

Working with unscaled data seems preferable, otherwise there is the risk of dramatically up-weighting components present in very small amounts and showing little variation (such as spectral background or baseline). However, it is desirable to give to different compounds a comparable influence in the data analysis, due to the presence of major and minor constituents. Thus, the data set was scaled using the block-scaling procedure called "block-adjusted non-scaled data".[56] In particular, NMR spectra were divided into different regions (blocks) whose values were scaled to attain the same block-variance after pretreatment. The block regions and the pretreated signals are reported in Figure 1.

PCA, as a first explorative tool, was carried out on a data set organized as a bidimensional matrix of 31 (human colon samples) × 6341 points (ppm). Four samples seemed to behave as outliers from PCA: samples c15 and c15t, that were not acquired with water-presaturation, and samples c17 and c17t, that showed a high signal at 2.0 ppm (correlating with a carbon at 21.1 ppm and probably due to sialic acid derivatives, not present in the other samples). Thus, these samples were excluded and PCA analysis was carried out on the reduced data array of dimension 27 samples (9 healthy, 9 neoplastic, and 9 macroscopically normal tissues) × 6341 points, that is, δ 9.05−0.05 ppm. PLS-DA was applied to discriminate healthy (9 samples) from neoplastic (9 samples) class, while macroscopically normal tissues (9 samples) were not used to build the PLS-DA model but projected on it afterward.

Six spectra acquired on 3 different patient tissues (3 spectra belonging to neoplastic and 3 to macroscopically/histologically normal tissues) were used as a test-set to validate and test the performance of the different models.

PCA and PLS-DA analyses were carried out using PLS-Toolbox 4.1 for MATLAB (distributed by eigenvector Research, WA).

The samples from healthy subjects are labeled in the text as c*x*, where *x* is a number corresponding to the subject, those from unhealthy subjects are labeled as c*x*t, when obtained from the lesion, and c*x**, when obtained at least 15 cm from the lesion. The six samples (3 unhealthy subjects: 3 samples obtained from the lesion and 3 at least 15 cm from the lesion) used as test-set are unlabeled. Data deriving from the same patient can thus be compared.

Results

Representative *ex vivo* HR-MAS 1D ^{1}H NMR spectra of healthy colorectal tissue (c2) are shown in Figure 2: trace 2a displays a conventional 1D ^{1}H HR-MAS NMR spectrum with water presaturation. This spectrum highlights both narrow and broad signals, which can be separated using a CPMG spin−echo (trace 2b) and a diffusion-edited sequence (trace 2c). The former shows signals due to the resonances of small metabolites, whereas the latter contributions from mobile lipids and macromolecules. The CPMG spectra of the healthy colorectal tissues display the presence of amino acids [alanine (Ala), valine (Val), leucine (Leu), isoleucine (Ile) and glutamate (Glu)], osmolites [lactate (Lac), taurine (Tau), creatine (Cr) and choline-containing compounds (ChoCC)] and polyols [*myo*-inositol (Myo) and *scyllo*-inositol (Scy)]. It is possible

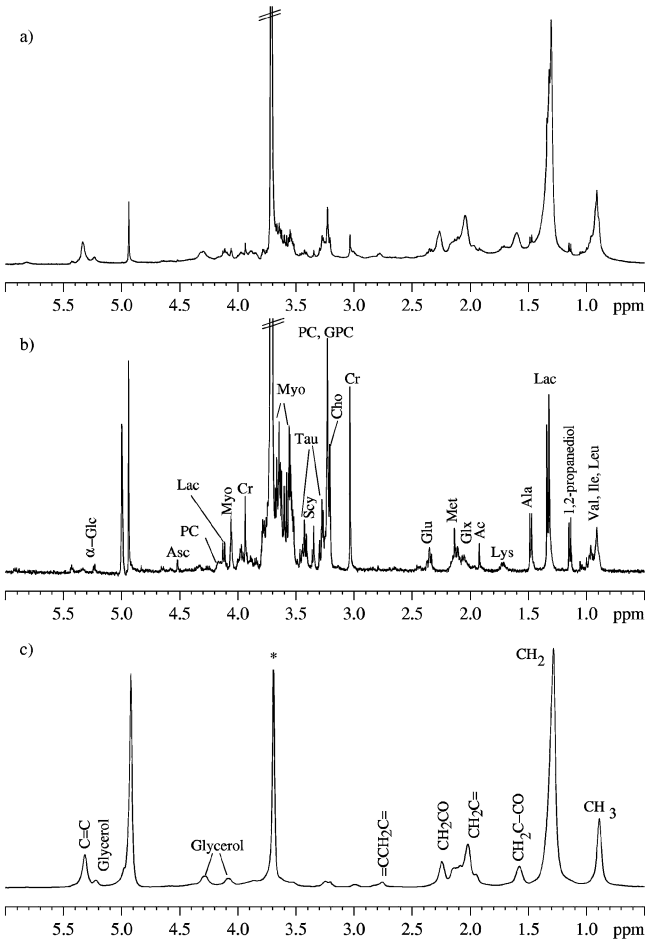

Figure 2. Representative *ex vivo* HR-MAS ^{1}H NMR spectra of healthy colorectal biopsy (c2) collected at endoscopy: (a) water-presaturated pulse sequence with composite pulse; (b) CPMG spectrum and (c) diffusion-edited spectrum (*). The strong signal at 3.72 ppm present in different amounts in some samples is due to PEG, used for colon preparation (PC = phosphorylcholine).

by inspecting the diffusion-edited spectra, to assign resonances mainly due to fatty acid chains and glycerol in triglycerides (TG), but also to macromolecules, as already observed in other human tissues.[16−18,32−34]

The assignment of metabolites is based on the analysis of 1D ^{1}H, and selected 2D (COSY, TOCSY and HSQC, see Supporting Information) NMR spectra. The obtained data are compared with those from the literature[32−34,57] and, when possible, with the experimental spectra that can be found in the Human Metabolome Database,[58] and assigned to the different metabolites. COSY and TOCSY spectra are very effective for the identification of coupling networks and hidden resonances: COSY spectra enable coupled proton−proton pairs to be found, whereas the TOCSY spectra permit ^{1}H,^{1}H connectivities up to five or six bonds and metabolite spin systems to be identified. HSQC spectra reveal directly bonded carbon−proton pairs, thus, enabling the assignment of singlets (which do not give correlations in homonuclear COSY and TOCSY spectra), and the discrimination among compounds having similar proton but diverse ^{13}C chemical shifts. All the experiments provide a complete and unambiguous identification of the metabolic pattern of the examined tissues. The main metabolites characterizing the colorectal tissues are labeled in Figure 2 and the pool of metabolites, especially osmolites, free amino acids, and mobile lipids (nearly 50), are reported in Table 2.

The NMR spectra of neoplastic and macroscopically/histologically normal colorectal tissues present different metabolic profiles toward those of the healthy ones. Furthermore, different metabolic profiles were also detected for the same tumor subtypes. Figure 3 (left) shows, as examples, the spectra of two adenocarcinoma subtypes. Spectra c12t and c14t derive from two patients affected by mild differentiated adenocarcinomas, whereas spectra c13t and c18t are from two patients affected by poorly differentiated adenocarcinomas.

Inspection of these spectra suggests that there is a great variability among these samples. Spectrum c12t (mild differentiated adenocarcinoma) is characterized by a predominant amount of lipids, in particular TG, whereas spectra c14t (mild differentiated adenocarcinoma) and c13t (poorly differentiated adenocarcinoma) reveal small metabolites, besides the presence of lipids. Spectrum c18t (poorly differentiated adenocarcinoma) shows the presence of metabolites and macromolecules, and the absence of lipids.

The spectra of the corresponding macroscopically/histologically normal colon specimens, collected during surgery at least 15 cm from the adenocarcinoma of the same patients, are reported in Figure 3 (right). The metabolic profiles are quite different also for this group of spectra, even though the samples are all classified as normal by histological analysis. The comparison with the corresponding neoplastic tissues hardly reveals any systematic difference. In fact, spectrum c12* (normal) is quite similar to c12t; c18* (normal) displays an increased amount of TG at a different percentage with respect to c18t, whereas c13* (normal) shows the absence of TG, in contrast to the other samples obtained at least 15 cm from the adenocarcinoma. A certain variability is also observed within the class of healthy samples (not shown).

We can conclude that all three classes of colorectal tissues here studied (neoplastic, histologically normal, and healthy) are characterized by a certain degree of metabolic heterogeneity, also within the same subclass of tumors. A statistical multivariate analysis of *ex vivo* HR-MAS NMR data may thus be helpful to find metabolic markers of the healthy and neoplastic state of colorectal tissues, and to classify the samples.

PCA was applied to the pretreated data set, to extract as much information as possible from the standard proton HR-MAS NMR spectra. We chose to model the standard ^{1}H presaturated spectrum instead of a CPMG spectrum, because it is the real primitive spectrum of a sample and contains information that is the sum of those present in CPMG and in diffusion-edited spectra. A PCA model with 5 principal components (PCs) was chosen according to minimum root mean squares error in cross-validation (venetian blind, 6 cancelation groups as implemented[59] in the PLS Toolbox), the explained X-block variance is 88% in fit (R^2) and 75% in cross validation (Q^2). Despite the applied pretreatments, the variability captured by the PC1 and PC2 components is mainly due to lipids and macromolecules, and no clear discrimination, among the healthy/neoplastic sample categories, is found by looking at PC1 versus PC2 scores plot. Conversely, a partial discrimination, among the samples belonging to the different categories, can be observed by the analysis of the scores plots of PC3 versus PC4 versus PC5 (Figure 4a), and two different groups are detected. The first includes the healthy samples and the second one the neoplastic and macroscopically/histologically normal colon samples. Furthermore, the healthy samples seem to be mainly discriminated for the negative values of PC3 and positive values of PC4 and PC5. Although c3, c8, and c9 samples

Table 2. List of ^{1}H and ^{13}C Chemical Shift (δ, ppm) of Metabolites Found in HR-MAS Spectra of Human Colon Tissue[a]

entry	metabolite	δ ^{1}H	δ ^{13}C	assignment	entry	metabolite	δ ^{1}H	δ ^{13}C	assignment
1	Fatty acids	0.89	14.6	CH_3	**21**	Phosphorylethanolamine	3.23 (t)	41.1	NCH_2
		1.31	29.4−32.2	$(CH_2)_n$			4.00	61.1	OCH_2
		1.59−1.60	25.0	CH_2−C-C=O	**22**	Glycerophosphorylethanolamine	3.30 (t)		NCH_2
		2.05	27.8	CH_2−C=			4.12		OCH_2
		2.26	34.2	CH_2C=O	**23**	Choline	3.20 (s)	54.6	$N(CH_3)_3$
		2.78, 2.83	25.7	=C-CH_2−C=			3.53	68.2	NCH_2
		5.31, 5.33	128.4, 130.3	CH=CH			4.07	56.5	OCH_2
2	Isoleucine	0.94 (t)	11.7	δ-CH_3	**24**	Glycerophosphoryl-choline	3.22 (s)	54.7	$N(CH_3)_3$
		1.02 (d)	15.3	γ-CH_3			3.68		NCH_2
		1.29, 1.48	25.5	γ-CH_2			4.33		OCH_2
		1.97		β-CH	**25**	Phosphorylcholine	3.22 (s)	54.7	$N(CH_3)_3$
		3.69		α-CH			3.61	67.2	NCH_2
3	Leucine	0.95 (d)	21.4	δ-CH_3			4.17	58.6	OCH_2
		0.97 (d)	22.8	δ-CH_3	**26**	β-Glucose	4.65 (d)	96.7	1-CH
		1.70	24.8	γ-CH			3.26 (t)	75.1	2-CH
		1.72	40.5	β-CH_2			3.49	76.7	3,5-CH
		3.75	[b]	α-CH			3.40	70.1	4-CH
4	Valine	0.99 (d)	17.3	γ-CH_3			3.88	61.3	6-CH_2
		1.04 (d)	18.7	γ-CH_3	**27**	Taurine	3.26 (t)	48.1	SCH_2
		2.25	29.7	β-CH			3.42 (t)	36.2	NCH_2
		3.61	[c]	α-CH	**28**	Myoinositol	3.29 (t)	75.3	5-CH
5	Threonine	1.33 (d)	20.3	γ-CH_3			3.63 (t)	73.2	4,6-CH
		4.26	66.7	β-CH			3.53 (dd)	72.0	1,3-CH
		3.60 (d)	61.1	α-CH			4.06 (t)	72.9	2-CH
6	Lactate	1.33 (d)	20.3	CH_3	**29**	Scyllo-inositol	3.35 (s)	74.5	CH
		4.11 (q)	69.1	CH	**30**	α-Glucose	5.24 (d)	92.7	1-CH
7	1,2-Propane	1.14 (d)	18.5	CH_3			3.54	72.9	2-CH
	diol	3.89		CH			3.73	73.2	3-CH
		3.54, 3.52		CH_2			3.84	72.0	5-CH
8	Alanine	1.48 (d)	16.8	β-CH_3			3.78	61.3	6-CH_2
		3.79 (q)	51.2	α-CH	**31**	Glycine	3.56 (s)	42.3	CH_2
9	Lysine	3.04 (t)	39.8	ε-CH_2	**32**	PEG	3.72 (s)	70.3	
		1.73	27.3	δ-CH_2	**33**	Glycerol (in lipids)	4.10, 4.30	62.5	1,3-CH_2
		1.48	22.3	γ-CH_2			5.24	69.2	2-CH
		1.91	30.5	β-CH_2	**34**	Glycerols	3.57, 3.66	63.2	1-CH_2
		3.79 (t)	[b]	α-CH			3.81	72.7	2-CH
10	Arginine	3.24 (t)	41.4	δ-CH_2	**35**	UDPG	4.34		2-CHrib
		1.69	24.9	γ-CH_2			5.92		1-CHrib
		1.93	28.3	β-CH_2			5.90		5-CHur
		3.78 (t)	[b]	α-CH			7.87		6-CHur
11	Glutamate	2.35	34.3	γ-CH_2	**36**	Uracil	5.80		5-CHur
		2.06, 2.15	27.6	β-CH_2			7.53		6-CHur
		3.77 (t)	[b]	α-CH	**37**	Formiate	8.48 (s)		
12	Glutamine	2.48	31.7	γ-CH_2	**38**	NADH	8.21 (s)		
		2.14	27.1	β-CH_2	**39**	Tryptophane	7.73	110.3	4-CH
		3.79 (t)	[b]	α-CH			7.19		5-CH
13	Proline	3.43, 3.34	46.7	δ-CH_2			7.29		6-CH
		2.01	24.0	γ-CH_2			7.52		7-CH
		2.34, 2.07	29.2	β-CH_2	**40**	Adenine	8.18 (s)		8-CH
		4.12 (t)	61.8	α-CH			8.21 (s)		2-CH
14	Methionine	2.13 (s)	14.9	SCH_3	**41**	NAc	2.05 (s)	23.0	CH_3
		2.70 (t)	29.4	γ-CH_2	**42**	Acetate	1.92 (s)	23.8	CH_3
		2.25	30.5	β-CH_2	**43**	Succinate	2.41 (s)		CH_2
		3.87 (t)	57.4	α-CH	**44**	Ascorbic Acid	4.52	79.0	CH
15	Aspartic acid	2.68, 2.82	37.5	β-CH_2			4.02		CH
		3.90 (dd)	52.7	α-CH	**45**	Ethanol	1.18 (t)	17.5	CH_3
16	Asparagine	2.85, 2.96		β-CH_2			3.64 (q)	56.7	CH_2
		4.01 (dd)	51.9	α-CH	**46**	OH-butyrate	1.20 (d)	22.3	CH_3
17	Creatine	3.04 (s)	37.5	NCH_3			4.14		CH
		3.92 (s)	54.4	CH_2			2.28, 2.40		CH_2
18	Tyrosine	3.06, 3.20		β-CH_2	**47**	Bonded Ala	1.40	17.1	β-CH_3
		3.93 (dd)	57.0	α-CH			4.35	50.7	α-CH
		6.88	116.6	H*ortho*	**48**	Bonded	1.22	19.6	γ-CH_3
		7.18	131.7	H*meta*		Thr	4.30	[d]	
19	Phenylalanine	3.11, 3.28		β-CH_2	**49**	Bonded	0.89	21.3	
		3.98	57.8	α-CH		Leu	4.30	[d]	
		7.33	129.9	H*ortho*	**50**	Bonded	0.95	18.8	
		7.38	128.2	H*para*		Val	4.30	[d]	
		7.43	129.6	H*meta*	**51**	Bonded	2.03	29.9	
20	Ethanolamine	3.15 (t)	42.1	NCH_2		Glu	4.30	[d]	
		3.82 (t)	58.2	OCH_2					

[a] ^{1}H chemical shift are referred to alanine doublet at 1.48 ppm; ^{13}C chemical shift are referred to alanine at 16.8 ppm. [b] Cα probably contributes to the 3.77, 55.1 ppm cross-peak. [c] Cα probably contributes to the 3.61, 61.1 ppm cross-peak. [d] Cα probably contributes to the 4.30, 54.3 ppm cross-peak.

belong to the first group, they lie far away from it, above all for negative values of PC4. Within the neoplastic specimens and those obtained at the resection margins at least 15 cm from the adenocarcinoma groups, all the samples are very close, except for c13t, which is located in the healthy group. The six unknown samples, collected from three different patients to be used as a test-set, are correctly predicted by the model as not healthy samples, and they are very close to the adenocarcinoma group. To highlight better the different grouping, cluster analysis was applied considering PC3, PC4, and PC5 scores values (distance measure based on principal component scores adjusted to unit variance and by using the centroid

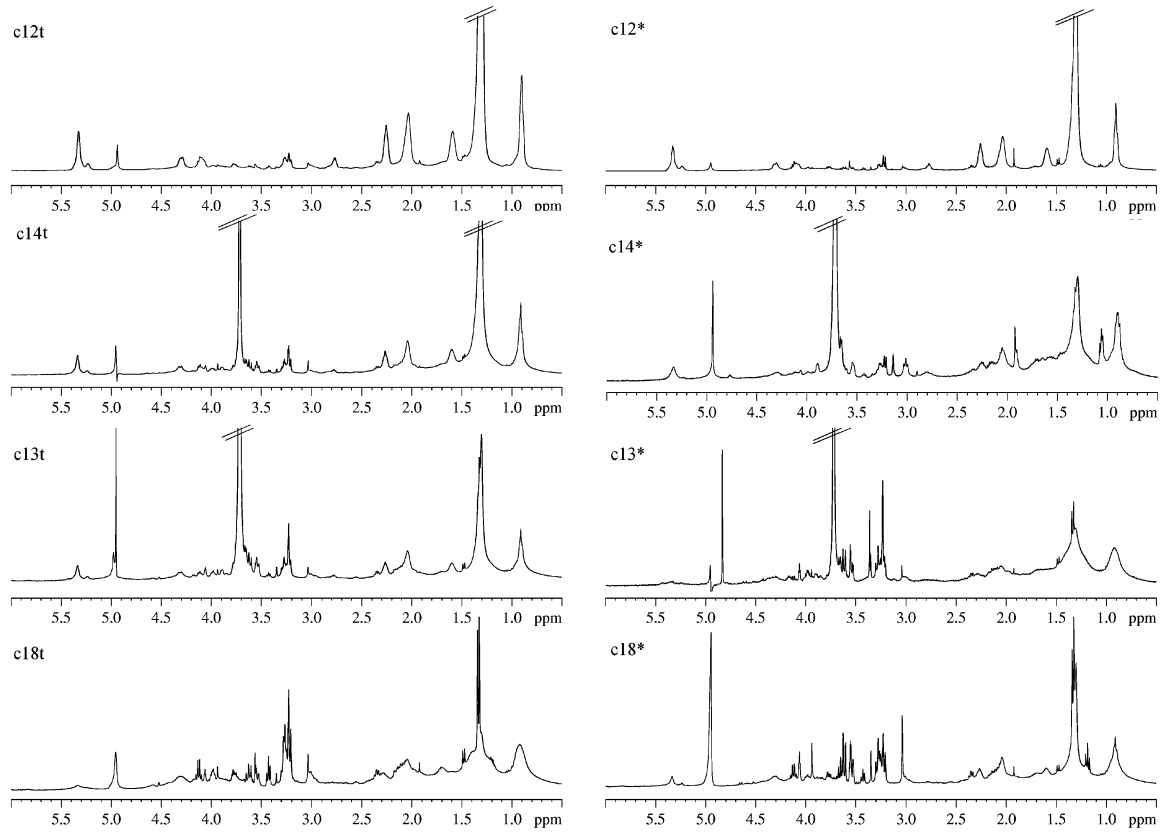

Figure 3. *Ex vivo* HR-MAS ^{1}H NMR water presaturated spectra of some colorectal biopsies. On the left: c12t and c14t from two different patients affected by mild differentiated adenocarcinomas, and c13t and c18t from two different patients affected by poorly differentiated adenocarcinomas. On the right: tissue specimens of macroscopically/histologically normal mucosa obtained at least 15 cm from the adenocarcinoma and from the same patients.

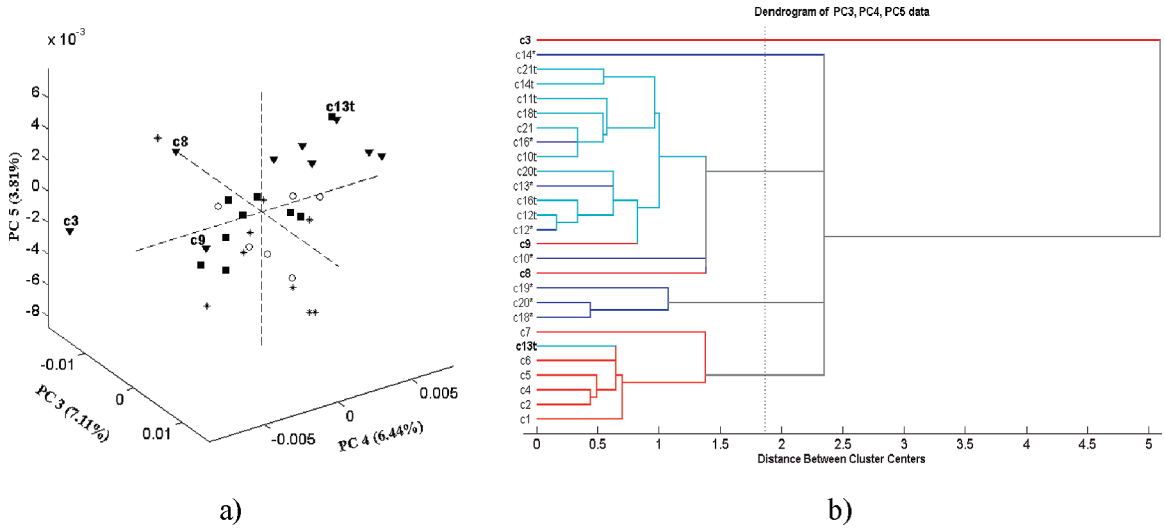

Figure 4. (a) Scores plot of PC3 vs PC4 vs PC5. (▼) Healthy samples, (■) adenocarcinomas, (*) specimens obtained at least 15 cm from the adenocarcinoma, and (○) unknown test samples. For clarity, only samples discussed in the text are labeled (according to Table 1 sample labels). (b) Dendrogram obtained by cluster analysis of PC3, PC4, and PC5 scores values. Red, healthy samples; light blue, adenocarcinomas; blue, specimens obtained at least 15 cm from adenocarcinomas.

method as linkage criterion). Figure 4b shows the obtained dendrogram, where healthy samples are depicted by red lines, neoplastic by light blue lines, and macroscopically/histologically normal colon samples by blue lines; it is evident that, apart from already discussed exceptions, that is, samples c3, c8, c9, and c13t, healthy and neoplastic samples form distinct clusters, whereas macroscopically/histologically normal colon samples are partly clustered with neoplastic samples and partly form their own cluster.

Zooms of the loadings plots of PC3, PC4, and PC5 versus the ppm region between 5.5 and 0.6 ppm are shown in Figure 5. The combined inspection of both scores and loadings plots (Figures 4 and 5) shows that the metabolic profile of healthy samples (negative PC3 scores values and positive PC4 and PC5)

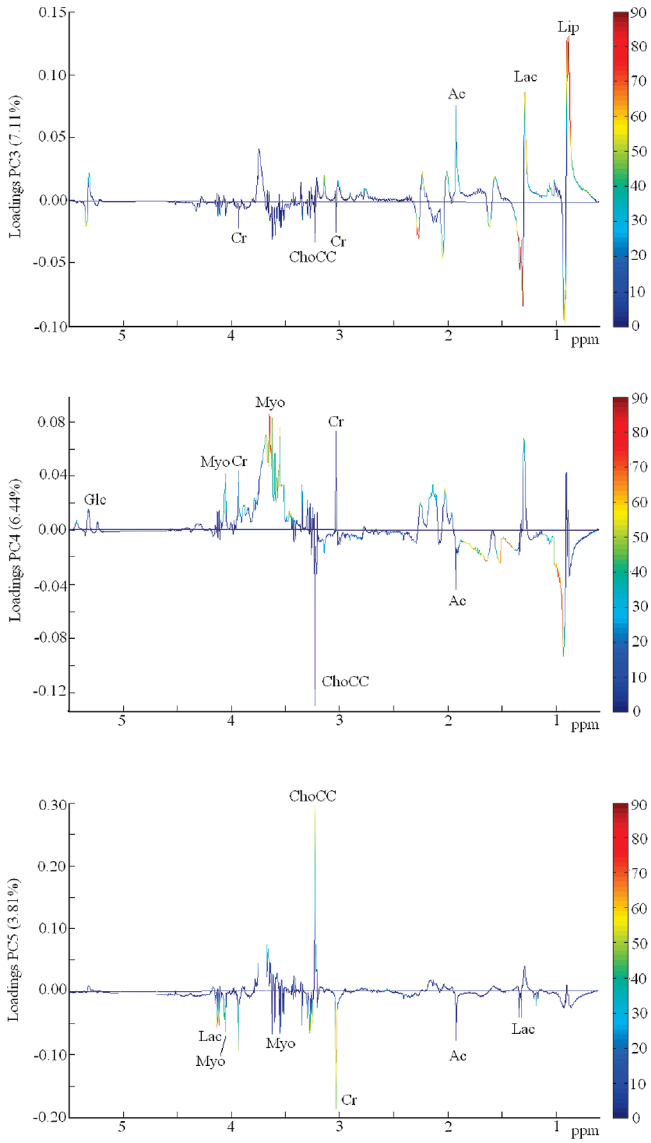

Figure 5. PC3, PC4, and PC5 loadings plots color coded according to percent variance captured for each variable. The abscissa has been represented in ppm to visualize better the metabolite resonances.

seems to be characterized by (i) low contribution of lipids (positive PC3 loadings in the 0.8−0.9 ppm region); (ii) high percentage of sugars and polyols (positive PC4 loadings), in particular Myo (positive PC4 loadings at 3.29, 3.53, 3.62 and 4.06 ppm), Scy (positive PC4 loadings at 3.35 ppm), glucose (Glc) (positive PC4 loadings at 3.54 ppm and 5.24−5.32 ppm region), and Cr (positive PC4 loadings in the region centered at 3.03 and 3.92 ppm); and (iii) high percentage of ChoCC (negative PC3 loadings and positive PC5 loadings at 3.22−3.23 ppm, characteristic of phosphorylcholine and GPC, while free Cho, at 3.20 ppm gives a minor contribution). The fact that ChoCC have negative loadings on PC4 (at 3.22−3.23 ppm) is only apparently contradictory. This is due to the different sign behavior on PC4 of samples c3, c8, and c9 that share a higher content of phosphorylcholine with the other healthy samples. Phosphorylcholine is characteristic for healthy samples and in c3 and c9; its content is higher with respect to all the other samples, both neoplastic and healthy. Neoplastic and most of the macroscopically/histologically normal specimens are characterized by an increased amount of lipids (positive PC3 loadings values in the 0.8−0.9 ppm region), and by the presence of acetate (Ac) (positive PC3 and negative PC4 and PC5 loadings values in the 1.92 ppm region). According to the observations previously made for healthy samples, the neoplastic ones are also characterized by decreased amount of sugars and polyols and by moderate ChoCC content. Samples c3 and c9 appear as outliers with respect to their own class, having negative PC4 and PC5 scores values (Figure 4) for their higher content of lipids. Sample c9 also shows a higher content of Ac with respect to the other healthy samples. On the other hand, c13t, mislocated near the healthy samples in scores plot (Figure 4), shows a higher amount of sugars, and a lower amount of lipids and Ac with respect to the other neoplastic samples.

To discriminate the predefined healthy and adenocarcinoma classes, the PLS-DA method was applied. A PLS-DA model was built using the NMR data as the dependent *X*-variables and class information as the *Y*-variables, that is, class 1, the 9 healthy samples, and class 2, the 9 adenocarcinoma ones. The optimal number of PLS-DA latent variables was determined predicting the "healthy" class of the colon tissues as shown in Figure 6. The calculated threshold above which samples are assigned to class 1 is shown as the horizontal dashed line. This threshold was estimated by using the Bayes Theorem[60] and was obtained by minimizing the total classification errors for the training set samples. All the healthy samples as well as eight of the nine belonging to the neoplastic class were correctly assigned; only one of the nine (c13t) was predicted as a borderline case. Furthermore, to assess the behavior of the model in estimating future samples, its performance was evaluated in cross validation (Figure 6, empty symbols). Three samples, two belonging to the healthy class ($c8_{CV}$ and $c9_{CV}$) and one to the tumoral one ($c13t_{CV}$), were misclassified. These are the same samples previously discussed as deviating with respect to their own class in explorative PCA analysis.

The test samples and macroscopically/histologically normal colon specimens were classified as belonging to adenocarcinoma class, since their predicted values were below the threshold value. It can be noticed that the macroscopically/histologically normal specimens generally shifted toward the healthy class, with respect to their corresponding tumoral tissues (compare c10*, c14*, c18*, c20* and c21* to c10t, c14t, c18t, c20t and c21t). These results indicate that the macroscopically/histologically normal colon tissues, while sharing some features with both the healthy and the neoplastic classes (as also suggested by the NMR spectral profiles), are more similar to the neoplastic class.

To identify the metabolites that mainly contribute to the achievement of good prediction or that influence the given model, the pseudo-regression coefficients plot (Figure 7) is reported together with average NMR spectra of healthy and tumoral samples, respectively. The values of the regression coefficients are directly correlated with their influences in the prediction ability of the model, whereas their sign is related to the discrimination class: positive coefficients associated with high *y*-values identify the healthy class, and negative coefficients identify the adenocarcinoma class.

The PLS-DA regression coefficients plot shows the same regions already highlighted as relevant by inspecting PCA loadings (Figure 5): negative contribution from lipids, Ac and Lac, characteristic of the neoplastic samples, and positive contributions from ChoCC, Cr and sugars, characteristic of the healthy class. In addition, there is a further contribution in the

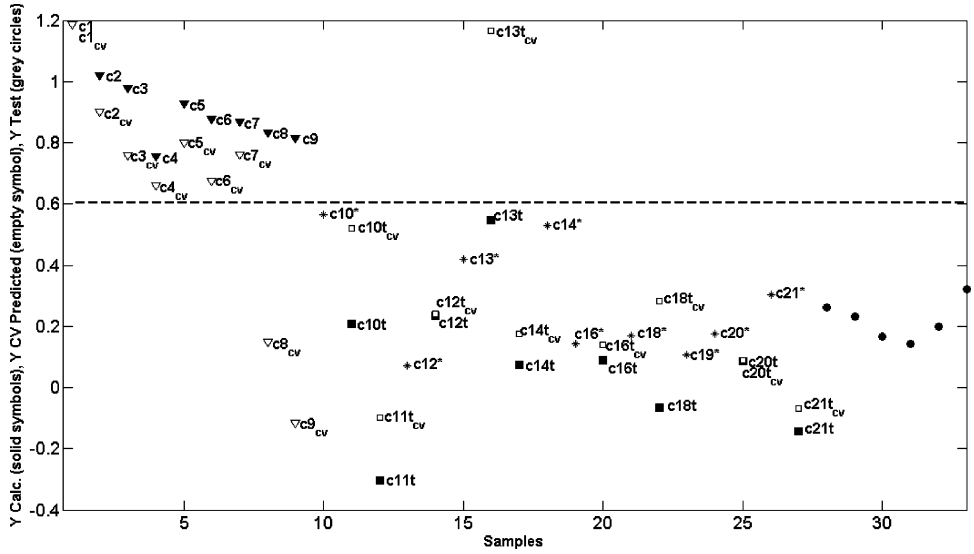

Figure 6. *Y* calculated, Y_{CV} predicted, and *Y* predicted vs number of samples (PLS-DA 3 latent variables). (▼) Healthy samples, (▽) healthy samples predicted in cross validation, (■) adenocarcinomas, (□) adenocarcinomas predicted in cross validation, (*) macroscopically/histologically normal colorectal specimens obtained at least 15 cm from the adenocarcinoma and (●) unknown samples. The dashed line shows the threshold value above which samples are assigned to class 1, that is, healthy samples. The samples are labeled as reported in Data Handling, in particular samples predicted in cross validation have the 'CV' specification as lower case.

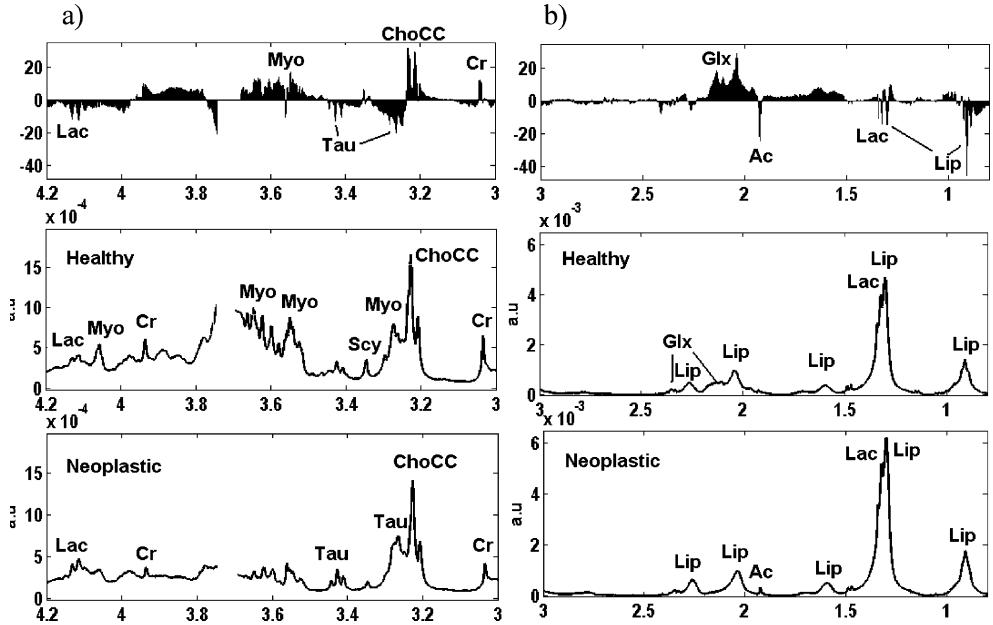

Figure 7. For the sake of clarity, zooms of regions (a) from 4.2 to 3 ppm and (b) from 3 to 0.8 ppm are reported. (Top) PLS-DA regression coefficients vs ppm; (middle) average NMR spectra of healthy; (bottom) average NMR spectra of neoplastic colon tissues.

discrimination of healthy and neoplastic colon classes from Tau (at 3.26 and 3.42 ppm) that has negative PLS-DA regression coefficients, and is reduced in the healthy class with respect to the neoplastic one, and from Glu and Gln (at 2.04−2.15 and 3.7−3.8 ppm) that have positive PLS-DA regression coefficients, and are increased in the healthy class with respect to the neoplastic one.

A closer inspection of the average NMR spectra of the healthy and neoplastic samples (Figure 7, middle and bottom) confirms the findings of PLS-DA analysis: neoplastic tissues are richer in Tau, Ac, Lac and lipids, whereas healthy tissues are richer in ChoCC, Cr, Glu plus Gln, polyols (Myo and Scy) and Glc.

Discussion

The metabolic profile of human colon tissue specimens, obtained through HR-MAS NMR, was analyzed with multivariate methods, to identify some molecular characteristics of adenocarcinomas.

The results obtained from multivariate data analysis shows that (i) just by looking at the NMR data, without imposing any classification model (unsupervised PCA), a partial distinction in two groups healthy and neoplastic together with macroscopically/histologically normal colorectal specimens (obtained at least 15 cm from the adenocarcinoma) is observed not in PC1 and PC2, but in PC3, PC4, and PC5; thus, a wide variability,

not linked to healthy-neoplastic differentiation, is present in the metabolic pattern, as captured by PC1 and PC2. This unsystematic variability is mainly due to lipids and macromolecules. Notwithstanding lipids are present in higher amount in neoplastic samples (as seen in PC3 loadings, and further confirmed by PLS-DA analysis, that is, regression coefficients plot, Figure 7), they are also responsible for the behavior of most of deviating samples, for example, c3, c9 and c13t, thus, indicating that, if considered alone, they are not a sufficient marker of the neoplastic state. (ii) By forcing a classification model on the basis of the training set samples (supervised PLS-DA), a better discrimination of the two classes was achieved, both in fit and cross validation (only three misclassified samples, two healthy, assigned to the neoplastic class, and one neoplastic, assigned to the healthy class, already seen as anomalous in PCA), and noticeably, the three neoplastic test samples (PLS-DA model used in prediction) were correctly recognized; all the macroscopically/histologically normal colon specimens (the nine samples labeled by asterisk (*) in Table 1 plus the three belonging to the test set) were predicted as belonging to adenocarcinoma class. (iii) Colorectal adenocarcinoma and macroscopically/histologically normal tissue samples are characterized by decreased levels of ChoCC, Cr, Glu plus Gln, polyols (Myo and Scy), Glc and increased levels of Tau, Ac, Lac and lipids, with respect to healthy colorectal tissues. The macroscopically/histologically normal samples are not intermediate between normal and malignant tissues but are more similar to neoplastic ones.

Our data obtained from healthy specimens are complementary to those reported by Nicholson's group for healthy colonic mucosa,[36] which was characterized by higher contents of Ac, Glu, Myo and Scy, Lac and lower contents of Cr, GPC and Tau with respect to the other regions of the GIT.

The significant increase in Tau levels in colon adenocarcinomas might be a good discrimination between normal and carcinomatous colorectal tissues, according to what reported by Arus et al.,.[61] This increase might be related to a more active metabolism and tumor aggressiveness in CRC[62] and stimulation of glycolysis,[63] since there is a high energetic demand from the neoplastic cells.

Myo is an important metabolite in regulating vital cellular functions such as transduction signal, cell proliferation, and differentiation.[64] It is also a component of cell membranes, and an essential nutrient required by human cells for growth and survival. Reduced Myo in colon tumoral tissues is due to the loss of differentiation of the neoplastic cells with respect to the normal mucosa and may also be a response to the increased Tau levels, according to Arùs et al.[65]

Lac proved to be useful in discriminating colorectal adenocarcinomas and healthy mucosa. Neoplastic colorectal lesions metabolize glucose (which decreases in adenocarcinomas) to lactate,[66] as observed in the large intestine when compared with the other regions of the human gastrointestinal tract.[36] The possibility that Lac can be produced from anaerobic glycolysis during *ex vivo* HR-MAS NMR acquisition has been ruled out in previous studies.[32,67] It should also be considered that Lac content increases in hypoxic tumoral tissues.[68] The lactate pool has also been found to be metabolically active in most cancers,[69] including colorectal carcinomas,[70] for which an anaerobic metabolism has been suggested with increased glucose absorption and lactate extrusion.

Cancer has a significantly altered choline phospholipid metabolism compared with normal tissue,[71] and an increase in phosphorylcholine and other ChoCC characterizes the aberrant choline phospholipid metabolism in cancers, as demonstrated by a number of NMR studies.[72−76] Conversely, our spectroscopic and chemometric data clearly show that lower levels of ChoCC are molecular characteristics both for the colorectal adenocarcinomas or the macroscopically/histologically normal mucosa at least 15 cm from the tumoral lesion. Similarly, a significant decrease in choline containing metabolites has been recently reported for rat pancreatic cancer.[77]

Lipids are present both in normal and neoplastic colon tissues, their amount being greater in the latter. The increase in lipid content is not so important as observed in human gastric adenocarcinoma,[33,34] where the presence of a high amount of lipids can be used as the most effective discriminating marker between normal and adenocarcinoma tissues.

In conclusion, despite the high degree of metabolic heterogeneity highlighted by *ex vivo* HR-MAS NMR spectroscopy, the combination of NMR data with multivariate analysis shows significant differences in the metabolic profile of healthy tissues with respect to neoplastic and macroscopically normal ones. We were able to confirm that high levels of Tau, Ac, Lac and lipids, and low levels of ChoCC, Cr, Glu plus Gln, polyols (Myo and Scy), and Glc are molecular characteristics of the colon adenocarcinoma tissues. Moreover, it is important to note that the multivariate statistical analysis suggests that macroscopically/histologically normal specimens obtained at least 15 cm from the adenocarcinoma are more similar to neoplastic than healthy tissue, thus, suggesting that the NMR spectroscopy is sensitive in detecting premalignant metabolic features before the appearance of morphological changes.[7−9]

NMR and chemometrics might offer useful information for the diagnosis of colorectal cancer, but in this respect, it is necessary to extend the study to a large number of samples to validate the discrimination among different types and grades of adenocarcinoma, to assess the clinical significance of *ex vivo* HR-MAS NMR and to obtain useful data for noninvasive clinical applications of *in vivo* NMR spectroscopy.

Abbreviations: Ala, alanine; Arg, arginine; -Ala-, bonded alanine; -Thr-, bonded threonine; CPMG, Carr−Purcell−Meiboom−Gill; ChoCC, choline-containing compounds; CRC, colorectal cancer; COSY, COrrelation SpectroscopY; Cr, creatine; Cho, free choline; Glc, glucose; Glu, glutamate; GPC, glycerophosphorylcholine; TG, triglycerides; HSQC, Heteronuclear Single Quantum Coherence; HR-MAS, High-Resolution Magic Angle Spinning; Ile, isoleucine; Lac, lactate; Leu, leucine; Lip, lipids; Lys, lysine; Myo, *myo*-inositol; PE, phosphoryletanolamine; PEG, polyethilenglycole; PCA, Principal Components Analysis; PLS-DA, Partial Least Squares Discriminant Analysis; Pro, proline; Scy, *scyllo*-inositol; Tau, taurine; TOCSY, TOtal Correlation SpectroscopY; Val, valine.

Acknowledgment. We greatly acknowledge The Fondazione Cassa di Risparmio di Modena for the financial support given for the acquisition of the Bruker Avance400 Spectrometer and the Centro Interdipartimentale Grandi Strumenti of the University of Modena and Reggio Emilia for the use of it. This research was supported by grants ex 60% from MIUR.

Supporting Information Available: More details on NMR assignments through TOCSY and HSQC. This material is available free of charge via the Internet at http://pubs.acs.org.

References

(1) Schulmann, K.; Reiser, M.; Schmiegel, W. *Best Pract. Res. Clin. Gastroenterol.* **2002**, *16*, 91–114.
(2) Pignone, M.; Rich, M.; Teutch, S. M.; Berg, A. O.; Lohr, K. N. *Ann. Intern. Med.* **2002**, *137*, 132–141.
(3) Smith, R. A.; Cokkinides, V.; von Eschenbach, A. C.; Levin, B.; Cohen, C.; Runowicz, C. D.; Sender, S.; Saslow, D.; Eyre, H. J. *CA Cancer J. Clin.* **2002**, *52*, 8–22.
(4) Ransohoff, D. F.; Sandler, R. S. *N. Engl. J. Med* **2002**, *346*, 40–44.
(5) Hartmann, D.; Bassler, B.; Schilling, D.; Adamek, H. E.; Jakobs, R.; Pfeifer, B.; Eickhoff, A.; Zindel, C.; Riemann, J. F.; Layer, G. *Radiology* **2006**, *238*, 143–149.
(6) Kuehle, C. A.; Langhorst, J.; Ladd, S. C.; Zoepf, T.; Nuefer, M.; Grabellus, F.; Barkhausen, J.; Gerken, G.; Lauenstein, T. C. *Gut* **2007**, *56*, 1079–1085.
(7) *Nuclear Magnetic Resonance Spectroscopy in the Study of Neoplastic Tissue*; Tosi, M. R., Tugnoli, V., Eds.; Nova Science Publishers, Inc.: New York, 2005.
(8) Gillies, R. J.; Morse, D. L. *Annu. Rew. Biomed. Eng.* **2005**, *7*, 287–326.
(9) Kwock, L.; Smith, J. K.; Castillo, M.; Ewend, M. G.; Collichio, F.; Morris, D. E.; Bouldin, T. W.; Cush, S. *Lancet Oncol.* **2006**, *7*, 859–868.
(10) Dzik-Jurasz, A. S.; Murphy, P. S.; George, M.; Prock, T.; Collins, D. J.; Swift, I.; Leach, M. O.; Rowland, I. J. *Magn. Reson. Med.* **2002**, *47*, 809–811.
(11) Cheng, L. L.; Chang, I.-W.; Louis, D. N.; Gonzalez, R. G. *Cancer Res.* **1998**, *58*, 1825–1832.
(12) Barton, S. J.; Howe, F. A.; Tomlins, A. M.; Cudlip, S. A.; Nicholson, J. K.; Bell, B. A.; Griffiths, J. R. *MAGMA* **1999**, *8*, 121–128.
(13) Cheng, L. L.; Anthony, D. C.; Comite, A. R.; Black, P. M.; Tzika, A. A.; Gonzalez, R. G. *Neuro-Oncology* **2000**, *2*, 87–95.
(14) Tzika, A. A.; Cheng, L. L.; Goumnerovan, L.; Madsen, J. R.; Zurakowski, D.; Astrakas, L. G.; Zarifi, M. K.; Scott, R. M.; Anthony, D. C.; Gonzalez, R. G.; Black, P. M. *J. Neurosurg.* **2002**, *96*, 1023–1031.
(15) Sitter, B.; Autti, T.; Tyynelä, J.; Sonnewald, U.; Bathen, T. F.; Puranen, J.; Santavuori, P.; Haltia, M. J.; Paetau, A.; Polvikoski, T.; Gribbestad, I. S.; Häkkinen, A. M. *J. Neurosci. Res.* **2004**, *77*, 762–769.
(16) Martinez-Brisbal, M. C.; Marti-Bonmati, L.; Piquer, R. J.; Revert, A.; Ferrer, P.; Llacer, J. L.; Piotto, M.; Assemat, O.; Celda, B. *NMR Biomed.* **2004**, *17*, 191–205.
(17) Tugnoli, V.; Schenetti, L.; Mucci, A.; Nocetti, L.; Toraci, C.; Mavilla, L.; Basso, G.; Rovati, R.; Tavani, F.; Zunarelli, E.; Righi, V.; Tosi, M. R. *Int. J. Mol. Med.* **2005**, *16*, 301–307.
(18) Tugnoli, V.; Schenetti, L.; Mucci, A.; Parenti, F.; Cagnoli, R.; Righi, V.; Trinchero, A.; Nocetti, L.; Toraci, C.; Mavilla, L.; Trentini, G.; Zunarelli, E.; Tosi, M. R. *Int. J. Mol. Med.* **2006**, *18*, 859–869.
(19) Sjøbakk, E.; Johansen, T.; Bathen, R.; Sonnewald, T. F.; Juul, R.; Torp, S. H.; Lundgren, S.; Gribbestad, I. S. *NMR Biomed.* **2008**, *21*, 175–185.
(20) Sitter, B.; Sonnewald, U.; Spraul, M.; Fjosne, H. E.; Gribbestad, I. S. *NMR Biomed.* **2002**, *15*, 327–337.
(21) Bathen, T. F.; Jensen, L. R.; Sitter, B.; Fjösne, H. E.; Halgunset, J.; Axelson, D. E.; Gribbestad, I. S.; Lundgren, S. *Breast Cancer Res. Treat.* **2007**, *104*, 181–189.
(22) Sitter, B.; Lundgren, S.; Bathen, T. F.; Halgunset, J.; Fjosne, H. E.; Gribbestad, I. S. *NMR Biomed.* **2006**, *19*, 30–40.
(23) Celda, B.; Monleon, D.; Martinez-Bisbal, M. C.; Esteve, V.; Martinez-Granados, B.; Pinero, E.; Ferrer, R.; Piquer, J.; Marti-Bonmati, L.; Cervera, J. *Adv. Exp. Med. Biol.* **2006**, *587*, 285–302.
(24) Swanson, M. G.; Vigneron, D. B.; Tabatabai, Z. L.; Males, R. G.; Schmitt, L.; Carroll, P. R.; James, J. K.; Hurd, R. E.; Kurhanewicz, J. *Magn. Reson. Med.* **2003**, *50*, 944–954.
(25) Swanson, M. G.; Keshari, K. R.; Tabatabai, Z. L.; Simko, J. P.; Shinohara, K.; Carroll, P. R.; Zektzer, A. S.; Kurhanewicz, J. *Magn. Reson. Med.* **2008**, *60*, 33–40.
(26) Righi, V.; Mucci, A.; Schenetti, L.; Tosi, M. R.; Grigioni, W. F.; Corti, B.; Bertaccini, A.; Franceschelli, A.; Sanguedolce, F.; Schiavina, R.; Martorana, G.; Tugnoli, V. *Anticancer Res.* **2007**, *27*, 3195–3204.
(27) Garrod, S.; Humpfer, E.; Spraul, M.; Connor, S. C.; Polley, S.; Connelly, J.; Lindon, J. C.; Nicholson, J. K.; Holmes, E. *Magn. Reson. Med.* **1999**, *41*, 1108–1118.
(28) Tate, A. R.; Foxall, P. J.; Holmes, E.; Moka, D.; Spraul, M.; Nicholson, J. K.; Lindon, J. C. *NMR Biomed.* **2000**, *13*, 64–71.
(29) Sitter, B.; Bathen, T.; Hagen, B.; Arentz, C.; Skjeldestad, F. E.; Gribbestad, I. S. *MAGMA* **2004**, *16*, 174–181.
(30) Lyng, H.; Sitter, B.; Bathen, T. F.; Jensen, L. R.; Sundfor, K.; Kristensen, G. B.; Gribbestad, I. S. *BMC Cancer* **2007**, *17*, 7–11.
(31) Barba, I.; Jaimez-Auguets, E.; Rodriguez-Sinovas, A.; Garcia-Dorado, D. *MAGMA* **2007**, *20*, 265–271.
(32) Tugnoli, V.; Mucci, A.; Schenetti, L.; Calabrese, C.; Di Febo, G.; Rossi, M. C.; Tosi, M. R. *Int. J. Mol. Med.* **2004**, *14*, 1065–1071.
(33) Tugnoli, V.; Mucci, A.; Schenetti, L.; Righi, V.; Calabrese, C.; Fabbri, A.; Di Febo, G.; Tosi, M. R. *Oncol. Rep.* **2006**, *16*, 543–553.
(34) Calabrese, C.; Pisi, A.; Di Febo, G.; Liguori, G.; Filippini, G.; Cervellera, M.; Righi, V.; Lucchi, P.; Mucci, A.; Schenetti, L.; Tonini, V.; Tosi, M. R.; Tugnoli, V. *Cancer Epidemiol., Biomarkers Prev.* **2008**, *17*, 1386–1395.
(35) Seierstad, T.; Røe, K.; Sitter, B.; Halgunset, J.; Flatmark, K.; Ree, A. H.; Rune Olsen, D.; Gribbestad, I. S.; Bathen, T. F. *Mol. Cancer* **2008**, *7*, 33.
(36) Wang, Y.; Holmes, E.; Comelli, E. M.; Fotopoulos, G.; Dorta, G.; Tang, H.; Rantalainen, M. J.; Lindon, J. C.; Corthésy-Theulaz, I. E.; Fay, L. B.; Kochhar, S.; Nicholson, J. K. *J. Proteome Res.* **2007**, *6*, 3944–3951.
(37) Wang, Y.; Cloarec, O.; Tang, H.; Lindon, J. C.; Holmes, E.; Kochhar, S.; Nicholson, J. K. *Anal. Chem.* **2008**, *80*, 1058–1066.
(38) Lindon, J. C.; Holmes, E.; Nicholson, J. K. *Prog. NMR Spectrosc.* **2001**, *39*, 1–40.
(39) Cloarec, O.; Dumas, M. E.; Graig, A.; Barton, R. H.; Trygg, J.; Hudson, J.; Blancher, C.; Gauguier, D.; Lindon, J. C.; Holmes, H.; Nicholson, J. K. *Anal. Chem.* **2005**, *77*, 1282–1289.
(40) Trygg, J.; Holmes, E.; Lundstedt, T. *J. Proteome Res.* **2007**, *6*, 469–479.
(41) Craig, A.; Cloarec, O.; Holmes, E.; Nicholson, J. K.; Lindon, J. C. *Anal. Chem.* **2006**, *78*, 2262–2267.
(42) van der Berg, R. A.; Hoefsloot, H. C. J.; Westerhuis, J. A.; Smilde, A. K.; van der Werf, M. J. *BMC Genomics* **2006**, *7*, 142–156.
(43) Cloarec, O.; Dumas, M. E.; Trygg, J.; Craig, A.; Barton, R. H.; Lindon, J. C.; Nicholson, J. K.; Holmes, H. *Anal. Chem.* **2005**, *77*, 517–526.
(44) Maher, A. D.; Crockford, D.; Toft, H.; Malmodin, D.; Faber, J. H.; McCarthy, M. I.; Barrett, A.; Allen, M.; Walker, M.; Holmes, E.; Lindon, J. C.; Nicholson, J. K. *Anal. Chem.* **2008**, *80* (19), 7354–7362.
(45) Wold, S.; Esbensen, K. M.; Geladi, P. *Chemom. Intel. Lab. Syst.* **1987**, *2*, 37–52.
(46) Barker, M.; Rayens, W. *J. Chemom.* **2003**, *17*, 166–173.
(47) Schenetti, L.; Mucci, A.; Parenti, F.; Cagnoli, R.; Righi, V.; Tosi, M. R.; Tugnoli, V. *Concepts Magn. Reson., Part A* **2006**, *28A*, 430–443.
(48) Bax, A. *J. Magn. Reson.* **1985**, *65*, 142–145.
(49) Meiboom, S.; Gill, D. *Rev. Sci. Instrum.* **1958**, *20*, 688–691.
(50) Wu, D.; Chen, A.; Johnson, C. S., Jr. *J. Magn. Reson., Ser. A* **1995**, *115*, 260–264.
(51) Jeener, J. *Ampere International Summer School II*; Basko Polje: Yugoslavia, 1971.
(52) Aue, W. P.; Bartholdi, E.; Ernst, R. R. *J. Chem. Phys.* **1976**, *64*, 2229–2246.
(53) Braunschweiler, L.; Ernst, R. R. *J. Magn. Reson.* **1983**, *53*, 521–528.
(54) Bax, A.; Davis, D. G. *J. Magn. Reson.* **1985**, *65*, 355–360.
(55) Bodenhausen, G.; Ruben, D. J. *Chem. Phys. Lett.* **1980**, *69*, 185–189.
(56) Wold, S.; Johansson, E.; Cocchi, M. *3D QSAR in Drug Design: Theory, Methods, And Applications*; Kubinyi, H., Ed.; ESCOM Science Publischer: Leiden, 1993; p 523.
(57) Fan, T. W. M. *Prog. NMR. Spectrosc.* **1996**, *28*, 161–219.
(58) Wishart, D. S.; Tzur, D.; Knox, C.; Eisner, R.; ChiGuo, A.; Young, N.; Cheng, D.; Jewell, K.; Arndt, D.; Sawhney, S.; Fung, C.; Nikolai, L.; Lewis, M.; Coutouly, M.-A.; Forsythe, I.; Tang, P.; Shrivastava, S.; Jeroncic, K.; Stothard, P.; Amegbey, G.; Block, D.; Hau, D. D.; Wagner, J.; Miniaci, J.; Clements, M.; Gebremedhin, M.; Guo, N.; Zhang, Y.; Duggan, G. E.; MacInnis, G. D.; Weljie, A. M.; Dowlatabadi, R.; Bamforth, F.; Clive, D.; Greiner, R.; Li, L.; Marrie, T.; Sykes, B. D.; Vogel, H. J.; Querengesser, L. *Nucleic Acids Res.* **2007**, *35* (Database issue), D521–D526.
(59) Bro, R.; Kjeldahl, K.; Smilde, A. K.; Kiers, H. A. L. *Anal. Bioanal. Chem.* **2008**, *390*, 1241–1251.
(60) Wise, B. M.; Gallagher, N. B.; Bro, R.; Shaver J. M.; Windig, W.; Koch, R. S. *PLS_Toolbox 4.1 for use with MATLAB*; Software, Eigenvector Research, Inc.: Wenatchee, WA, 2007.
(61) Moreno, A.; Rey, M.; Montane, J. M.; Alonso, J.; Arus, C. *NMR Biomed.* **1993**, *6*, 111–118.
(62) Galons, J. P.; Fantini, J.; Vion-Dury, J.; Cozzone, P. J.; Canioni, P. *Biochimie* **1989**, *71*, 949–961.
(63) Bouckenooghe, T.; Remacle, C.; Reusens, B. *Curr. Opin. Clin. Nutr. Metab. Care* **2006**, *9*, 728–733.
(64) Vucenik, I.; Shamsuddin, A. M. *Nutr. Cancer* **2006**, *55*, 109–125.
(65) Moreno, A.; Arus, C. *NMR Biomed.* **1996**, *8*, 33–45.

(66) Budohoski, L.; Challis, R. A. J.; Newsholme, E. A. *Biochem. J.* **1982**, *206*, 169–172.
(67) Waters, N. J.; Garrod, S.; Farrant, R. D.; Haselden, J. N.; Connor, S. C.; Connelly, J.; Lindon, J. C.; Holmes, E.; Nicholson, J. K. *Anal. Biochem.* **2000**, *282*, 16–23.
(68) Preul, M. C.; Caramanos, Z.; Collins, D. L.; Villemure, J. G.; Leblanc, R.; Olivier, A.; Pokrupa, R.; Arnold, D. L. *Nat. Med.* **1996**, *2*, 323–325.
(69) Terpstra, M.; Gruetter, R.; High, W. B.; Mescher, M.; DelaBarre, L.; Merkle, H.; Garwood, M. *Cancer Res.* **1998**, *58*, 5083–5088.
(70) Koukourakis, M. I.; Giatromanolaki, A.; Harris, A. L.; Sivridis, E. *Cancer Res.* **2006**, *66*, 332–337.
(71) Podo, F. *NMR Biomed.* **1999**, *12*, 413–439.
(72) Aboyage, E. O.; Bujwalla, Z. M. *Cancer Res.* **1999**, *59*, 80–84.
(73) Glunde, K.; Jie, C.; Bhujwalla, Z. M. *Cancer Res.* **2004**, *64*, 4270–4276.
(74) Iorio, E.; Mezzanzanica, D.; Alberti, P.; Spadaro, F.; Ramoni, C.; D'Ascenzo, S.; Millimaggi, D.; Pavan, A.; Dolo, V.; Canevari, S.; Podo, F. *Cancer Res.* **2005**, *65*, 9369–9376.
(75) Glunde, K.; Serkova, N. J. *Pharmacogenomics* **2006**, *7*, 1109–1123.
(76) Glunde, K.; Bhujwalla, Z. M. *Lancet Oncol.* **2007**, *8*, 855–857.
(77) Fang, F.; He, X.; Deng, H.; Chen, Q.; Lu, J.; Spraul, M.; Yu, Y. *Cancer Sci.* **2007**, *98*, 1678–1682.

PR801094B